

The Investigation of the hydrodynamic drag of a slit microchannel with a textured wall

© A.S. Lobasov^{1,2}, A.V. Minakov^{1,2}

¹ Siberian Federal University, Krasnoyarsk, Russia

² Kutateladze Institute of Thermophysics, Russian Academy of Sciences, Siberian Branch, Novosibirsk, Russia

E-mail: perpetuityrs@mail.ru

Received May 12, 2021

Revised September 10, 2021

Accepted September 19, 2021

The results of numerical investigation of the hydrodynamic drag of a slit microchannel with a textured wall surface, as well as of the pressure drop in such a channel and the effective slip length on the wall for various Reynolds numbers, are presented. The channel height was $10\mu\text{m}$, and the length varied from 25 to $500\mu\text{m}$. It was found that the pressure drop in the textured microchannel was less than in a conventional one at any length. The dependences of the relative pressure drop, friction factor, and effective slip length on the Reynolds number were obtained for various channel lengths. A correlation that describes the dependence of the relative pressure drop on the Reynolds number for small channel lengths was proposed. The friction factor was described by a correlation expressed as $20 / \text{Re}$.

Keywords: microchannel, textured wall, wall slip, numerical simulation

DOI: 10.21883/TPL.2022.01.52458.18866

Nanohydrodynamics is being intensely developed in recent years because of the miniaturization of devices in various fields of technology: aerospace industry, power engineering, electronics, transport and medicine, oil and gas industry. In addition, mini— and microchannels are widely spread in biological systems. However, in microchannels whose lateral sizes are very small, i.e., the walls are very close to each other, and, if no-slip conditions is fulfilled, the fluid velocity is also very small while the hydraulic drag is high. One of the possible solutions to this issue is exploiting the effect of wall slip which is that the fluid near-wall velocity becomes nonzero due to certain surface properties. One of the research fields of interest is studying surfaces to which microtextured layers of extremely high or extremely low wettability are applied with subsequent control of the wettability of those nanostructures. In recent years, it became possible to create microtextured materials with contact angles of about 150° , which possess such properties as self-cleaning, self-water-repellency, anti-icing and antifogging [1]. Moreover, various microfluidic devices are being developed at present: microscale thermophysical devices, bio-microelectromechanical systems and „lab-on-chip“ devices [2,3] exploiting the ultrahydrophobic properties. Therefore, in recent years, both abroad [1–5] and in Russia [6–10], there arose a great interest in investigating high— and superhydrophobic microtextured surfaces. Therefore, in this work, we have studied the effect of the slit textured microchannel length on the pressure drop in this channel, hydrodynamic drag factor, and effective wall slip length for different Reynolds numbers. The microchannel height was $10\mu\text{m}$, and the length ranged from 25 to $500\mu\text{m}$. This paper considers three-dimensional flows of incompress-

ible fluids described by using the hydrodynamic approach based on solving the Navier–Stokes equations system. This approach was considered in detail in [11], and only the main points of the numerical technique are noted below. In this paper, milestones of the numerical technique are presented below. The difference analogue of the convection-diffusion equations was found by means of the finite volume method for structured multiblock grids. The convective terms of the transfer equation were approximated by using upwind second-order schemes. The relations between the velocity and pressure fields ensuring the fulfilment of the continuity equation were realized using the SIMPLEC-procedure at aligned grids [12]. The difference equations obtained as a result of discretizing the initial system were solved iteratively using the algebraic multigrid solver. In this approach, periodic boundary conditions were set at the channel lateral walls; thus, the channel width was regarded as infinite. At the top wall, no-slip conditions were set. The bottom wall was a combination of textured sections with no-slip boundary conditions and free-surface sections simulating air cavities between the textures. In the free-surface sections, the wall slip of the flow was set based on the zero shear stress condition. The textured sections were squares with a side of $1\mu\text{m}$, they were arranged in the chessboard pattern with longitudinal and transverse steps also equal to $1\mu\text{m}$. At the microchannel inlet, a parabolic velocity profile was set, and the channel outlet remained free. The water with a viscosity of $0.001\text{ Pa}\cdot\text{s}$ and a density of 1000 kg/m^3 was used as a working fluid. The Reynolds numbers varied from 0.1 to 100 according to variations in the fluid mean flow rate.

The calculations showed that the pressure drop in the textured microchannel was lower than in an ordinary channel at any microchannel length and any Reynolds numbers. Due to this, the effect of the presence of textures on the microchannel wall may be estimated using a dimensionless ratio between the pressure drop in the channel free of textured walls and that in the channel with a textured wall. The dependence of this dimensionless criterion on the Reynolds number for different dimensionless channel lengths (channel length related to its height) is represented in Fig. 1. The figure shows that the relative pressure drop depends linearly on the Reynolds number, the straight-line slope decreasing with increasing relative channel length. This is apparently due to the microchannel top wall being nontextured, and friction losses increase on this wall with increasing channel length. In addition, even in the longest channel where the relative pressure drop is independent of the Reynolds number, it is approximately 1.2, i. e., the use of the textured wall enables a 20% reduction of hydrodynamic losses in such a channel.

Another no less important characteristic is the effective wall slip velocity defined as the ratio between the mean velocity on this wall and the mean velocity gradient on this wall: $l_{eff} = \langle u_s \rangle / \langle \delta u / \delta n \rangle$. The velocity gradient will be defined based on Newton's rheological law: $\langle \tau \rangle = -\mu(\delta u / \delta n)$. In its turn, shear stress $\langle \tau \rangle$ is proportional to the channel pressure drop. Finally, the effective slip length in the slit microchannel will be defined as follows: $l_{eff} = (2\langle u_s \rangle \mu l) / (\Delta p h)$, where μ is the fluid dynamic viscosity; l , h are the channel length and height, respectively; Δp is the pressure drop in the channel. Fig. 2 presents the effective wall slip length on the Reynolds number for different dimensionless channel lengths. One

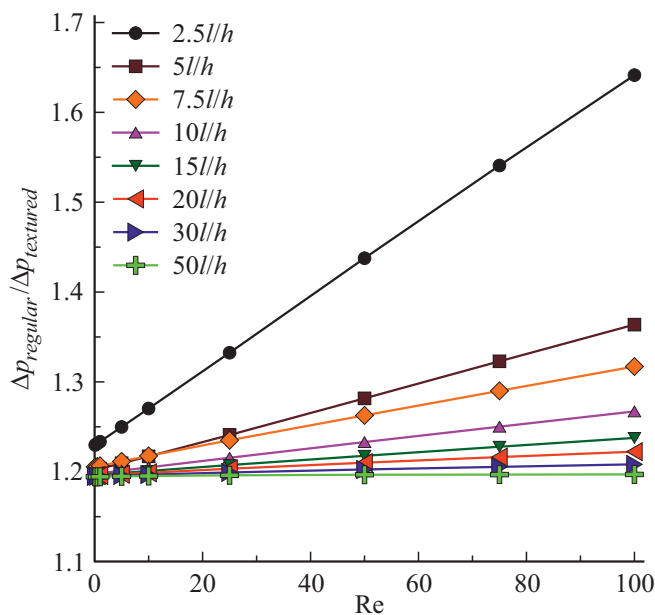


Figure 1. The dependence of the relative pressure drop in a microchannel on the Reynolds number for various relative lengths of such a microchannel.

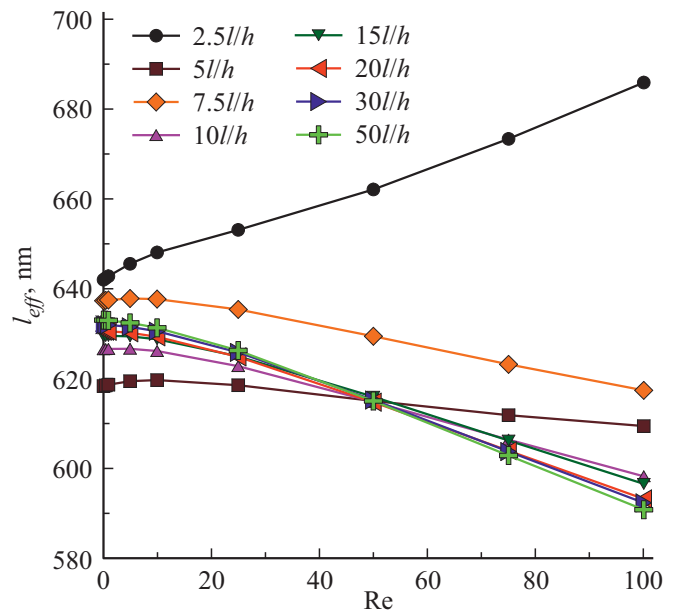


Figure 2. The dependence of the effective slip length on the microchannel wall on the Reynolds number for various relative lengths of such a microchannel.

can see that this quantity depends nonlinearly on both the Reynolds number and the reduced channel length. More detailed investigations of the effect of various parameters on this value will be carried out later. However, it is possible to reveal from this plot that the mean effective slip length is about 630 nm or 6.3% of the microchannel height.

Further, the influence of the the presence of texturing on the microchannel wall on the hydrodynamic friction factor was studied. Its dependence on the reduced channel length at different Reynolds numbers is represented in Fig. 3. According to the theory [13], the slit channel friction factor is equal to $24/Re$, namely, is to be a straight line in the frame of reference used in Fig. 3. One can see that at large values of reduced microchannel lengths this dependence is indeed a straight line, however, at small values of reduced channel lengths the dependence begins deviating from a straight line, and the larger the Reynolds number, the stronger this deflection. Moreover, even the straight sections are inconsistent with the oretical values of the friction factor: they are perfectly describable by relation $\lambda_{eff} = 20/Re$, which is represented in Fig. 3 by a dashed line for each relevant Reynolds number. It is not surprising that the hydrodynamic drag factor in the textured-wall microchannel is lower than that in the nontextured-wall microchannel by 20% since this fully complies with the above-presented results of analyzing the relative pressure drop dependence.

After processing all obtained results, the following correlation function describing the behaviour of the microchannel relative pressure drop was suggested:

$$\Delta p_{rel} = 5.69 \cdot 10^{-4} (l/h)^{-1.5} Re + 1.1 \cdot 10^{-2} (l/h)^{-0.8} + 1.19.$$

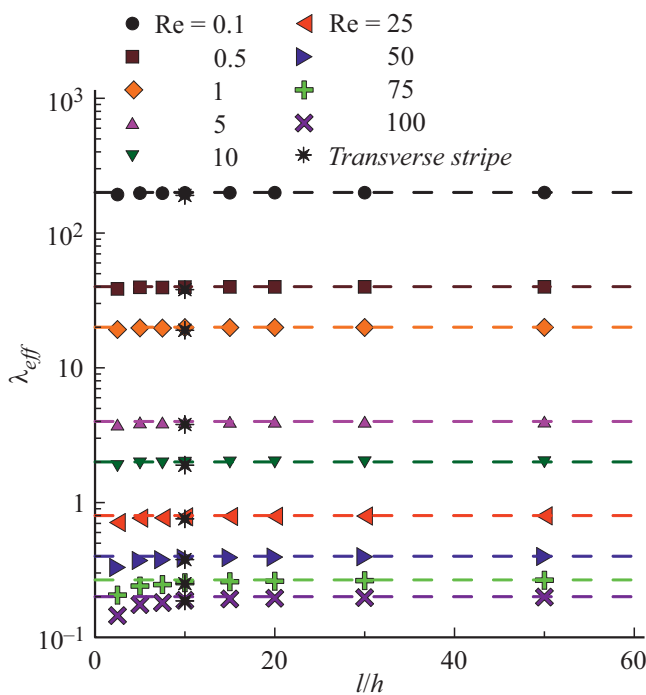


Figure 3. The dependence of the hydrodynamic friction factor on the relative length of the microchannel for various Reynolds numbers.

A comparison of the relative pressure drop obtained using this correlation with the calculations showed that the proposed correlation describes the obtained results with an accuracy of more than 95%. In addition, a different arrangement of texture sections was considered for a channel of $100\ \mu\text{m}$ long: the textures were made in the form of transverse stripes of $1\ \mu\text{m}$ wide with an inter-stripe distance of $3\ \mu\text{m}$. Thus, in this configuration the areas of textures and slip sections were equal to the ones of described above configuration. To compare them quantitatively, friction factors for the rough textures in the form of transverse stripes were additionally shown in Fig. 3. It is seen that the difference between values for two considered configurations decreases with an increase in Reynolds numbers, and it does not exceed 5% even at the lowest Reynolds number. Hence, the main influence on the reduction of the pressure drop in the channel comes from the relative area of the slip section, but not from the pattern of the rough textures arrangement on the surface.

Thus, the study has shown that the pressure drop in a textured microchannel is lower than in an ordinary channel independently of its length. In this case, the relative pressure drop has a linear dependence on the Reynolds number, and with an increase in the relative length of the channel, the slope of this straight line decreases. The study showed that the use of a textured wall allows one to reduce of the hydrodynamic loss in such a microchannel by at least 20%. The hydrodynamic friction factor has been determined, which can be sufficiently accurately described by the $20/\text{Re}$

correlation. A quite simple correlation was suggested, which describes the relative pressure drop dependence on the Reynolds number with an accuracy of more than 95% for different dimensionless channel lengths. A dependence of the effective wall slip length on the Reynolds number was obtained for different dimensionless channel lengths. The mean value of this quantity is about 630 nm or 6.3% of the channel height. It was established that the effective slip length depends nonlinearly on both the Reynolds number and reduced channel length. However, in order to answer the question about the mechanisms of influence of various parameters on this value, it is necessary to conduct additional systematic studies.

Financial support

The study was supported by the Russian Scientific Foundation (Project № 20-79-00231 „Investigation of the management of the superhydrophobic properties of microchannels walls to enhance the effectiveness of microfluidic equipment“).

Conflict of interests

The authors declare that they have no conflict of interests.

References

- [1] B. Bhushan, Y.C. Jung, K. Koch, *Phil. Trans. Roy. Soc. A*, **367** (1894), 1631 (2009). DOI: 10.1098/rsta.2009.0014
- [2] G. Bhutani, K. Muralidhar, S. Khandekar, *Interfac. Phenom. Heat Transfer*, **1** (1), 29 (2013). DOI: 10.1615/InterfacPhenomHeatTransfer.2013007038
- [3] H. Liu, L. Feng, J. Zhai, L. Jiang, D. Zhu, *Langmuir*, **20** (14), 5659 (2004). DOI: 10.1021/la036280o
- [4] H.B. Eral, D.J.C.M. 't Mannetje, J.M. Oh, *Colloid Polym. Sci.*, **291**, 247 (2013). DOI: 10.1007/s00396-012-2796-6
- [5] M.T.Z. Myint, G.L. Hornyak, J. Dutta, *J. Colloid Interface Sci.*, **415**, 32 (2014). DOI: 10.1016/j.jcis.2013.10.015
- [6] A.I. Ageev, I.V. Golubkina, A.N. Osipov, *Phys. Fluids*, **30** (1), 012102 (2018). DOI: 10.1063/1.5009631
- [7] A.I. Ageev, A.N. Osipov, *J. Phys.: Conf. Ser.*, **1141**, 012134 (2018). DOI: 10.1088/1742-6596/1141/1/012134
- [8] A.E. Muslimov, A.Sh. Asvarov, N.S. Shabanov, V.M. Kanevsky, *Pis'ma v ZhTF*, **46** (19), 15 (2020) (in Russian). DOI: 10.21883/PJTF.2020.19.50037.18371
- [9] A.I. Ageev, A.N. Osipov, *Fluid Dyn.*, **54** (2), 205 (2019). DOI: 10.1134/S0015462819020010
- [10] E.S. Asmolov, T.V. Nizkaya, O.I. Vinogradova, *Phys. Rev. E*, **98** (3), 033103 (2018). DOI: 10.1103/PhysRevE.98.033103
- [11] A.S. Lobasov, A.V. Minakov, V.V. Kuznetsov, V.Y. Rudyak, A.A. Shebeleva, *Chem. Eng. Process.: Process Intensific.*, **134**, 105 (2018). DOI: 10.1016/j.ccep.2018.10.012
- [12] S. Patankar, *Numerical heat transfer and fluid flow* (Hemisphere publishing corporation, Washington-New York-London, 1980).
- [13] L.G. Loitsyanskii, *Mechanics of Liquids and Gases* (Pergamon Press Ltd., London, 1966).